analytical chemistry

Article

pubs.acs.org/ac

4-Phenyl-α-cyanocinnamic Acid Amide: Screening for a Negative Ion Matrix for MALDI-MS Imaging of Multiple Lipid Classes

Annabelle Fülöp,[†,‡,§] Martina B. Porada,[†,∥] Christian Marsching,[†,‡,§,⊥] Henning Blott,[†,∥] Björn Meyer,[†,‡,§] Suparna Tambe,[†,∥] Roger Sandhoff,[†,‡,⊥] Hans-Dieter Junker,[†,∥] and Carsten Hopf*[,†,‡,§]

[†]Applied Research Center in Biomedical Mass Spectrometry (ABIMAS), [‡]Instrumental Analysis and Bioanalysis, Mannheim University of Applied Sciences, Paul-Wittsack-Strasse 10, 68163 Mannheim, Germany

[§]Institute of Medical Technology, University of Heidelberg and Mannheim University of Applied Sciences, Paul-Wittsack-Strasse 10, 68163 Mannheim, Germany

[∥]Organic Chemistry, Aalen University of Applied Sciences, Beethovenstrasse 1, 73430 Aalen, Germany

[⊥]Lipid Pathobiochemistry, German Cancer Research Center (DKFZ), Im Neuenheimer Feld 280, 69120 Heidelberg, Germany

Supporting Information

ABSTRACT: Matrix-assisted laser desorption/ionization imaging mass spectrometry (MALDI-IMS) has become a method of choice in lipid analysis, as it provides localization information for defined lipids that is not readily accessible with nonmass spectrometric methods. Most current MALDI matrices have been found empirically. Nevertheless, preferential matrix properties for many analyte classes are poorly understood and may differ between lipid classes. We used rational matrix design and semiautomated screening for the discovery of new matrices suitable for MALDI-IMS of lipids. Utilizing Smartbeam- and nitrogen lasers for MALDI, we systematically compared doubly substituted α-cyanocinnamic acid derivatives (R^1-CCA-R^2) with respect to their ability to serve as negative ion matrix for various brain lipids. We identified 4-phenyl-α-cyanocinnamic acid amide (Ph-CCA-NH_2) as a novel negative ion matrix that enables analysis and imaging of various lipid classes by MALDI-MS. We demonstrate that Ph-CCA-NH_2 displays superior sensitivity and reproducibility compared to matrices commonly employed for lipids. A relatively small number of background peaks and good matrix suppression effect could make Ph-CCA-NH_2 a widely applicable tool for lipid analysis.

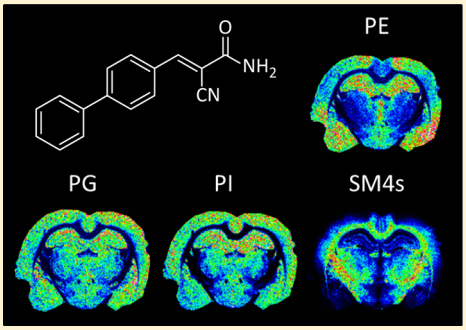

Lipids are major building blocks of biological membranes, and they play key roles in signal transduction pathways[1,2] and mechanisms of disease.[3,4] Because of these important functions, the field of lipid analysis and lipidomics has made considerable progress in recent years.[5,6] Matrix-assisted laser desorption/ionization time-of-flight mass spectrometry (MALDI-TOF MS)[7] in general and MALDI imaging MS (MALDI-IMS)[8,9] in particular, which provides information about the location of different lipid species, have become methods of choice for lipid studies.[10−14] In a typical MALDI-IMS experiment, a thin tissue cryosection is mounted onto a suitable target and covered with a chemical matrix solution that extracts analytes of interest from the underlying tissue. Some matrices limit the reproducibility and the spatial resolution of MALDI imaging experiments because of large or inhomogeneous crystal formation on the tissue slices. In addition, inhomogeneous cocrystallization of analytes with matrices can lead to the existence of so-called hot spots[15] on the sample, which causes quantitative errors and complicates automated measurement. Therefore, the role of the matrix is to cocrystallize with analytes and to absorb laser energy, in order to promote desorption/ionization. The challenges in imaging stem from the wide range of lipid concentrations and the very different ionization efficiencies of various lipid species. It is therefore necessary to choose a matrix that is either selective for a defined class of lipids[16,17] or that facilitates efficient ionization of a maximum number of lipid classes independent of their distinct physicochemical properties. In addition, a suitable matrix should possess a high absorbance at the emission wavelength of the laser and a low matrix background.[18,19] The presence of alkali metal ions in tissue slices leads to formation of multiple adducts for each lipid species in MALDI images in positive ion mode and thus complicates their interpretation. In contrast, in negative ion spectra the exclusive presence of $[M - H]^-$ ion signals formed from a large variety of lipids facilitates the analysis.

The most frequently used matrices for lipid MALDI-IMS in negative ion mode are 2,5-dihydroxybenzoic acid (DHB)[20] and 9-aminoacridine (9-AA).[17,21] However, DHB tends to form large crystals, which may cause molecular delocalization and poor spot-to-spot reproducibility,[22,23] and it exhibits only poor analyte sensitivities accompanied by strong background noise in

Received: June 17, 2013
Accepted: August 28, 2013
Published: August 28, 2013

   dx.doi.org/10.1021/ac4018154 | *Anal. Chem.* 2013, 85, 9156−9163

negative ion mode.[24] Therefore, it is not an ideal matrix for lipid detection in negative ion mode. Additional lipid matrices that have been used for negative ion MALDI-MS are 2,6-dihydroxyacetophenone (DHA),[25,26] 2-(2-aminoethylamino)-5-nitropyridine (AAN),[27] and 2-mercaptobenzothiazole (MBT).[28] However, the sublimation of DHA under high-vacuum conditions[29] presents a significant disadvantage for IMS, whereas the lipid signals of MBT and AAN in negative ion mode are weaker than those with 9-AA.[30]

Nearly all matrices in use today have been found empirically. Among the few exceptions are the rationally designed matrix 1,8-bis(dimethylamino)naphthalene[31] for the ionless detection of small molecules and the matrix 4-chloro-α-cyanocinnamic acid (Cl-CCA).[32] However, the replacement of the hydroxyl group in the conventional matrix 4-hydroxy-α-cyanocinnamic acid (HCCA) against the chlorine substituent leads to a hypsochromic shift. Consequently, increased performance is only achieved with MALDI-MS instruments with a nitrogen laser (337 nm) but not in instruments with a frequency-tripled Nd:YAG laser (355 nm).[32] Nevertheless, some substance properties (e.g., vacuum stability, crystallization) are hard to plan.

Here, we therefore rationally designed HCCA analogs with two substitutents (R^1-CCA-R^2) and performed semiautomated screening of various substances with respect to their utility as negative ion matrices for MALDI-MS analysis of brain lipids. In order to facilitate future use of these novel matrices in diverse applications, we provide performance measures in positive and negative ion mode utilizing nitrogen and Nd:YAG lasers as a resource for the lipid analysis community. Finally, we present 4-phenyl-α-cyanocinnamic acid amide (Ph-CCA-NH_2) as a novel MALDI-IMS matrix for analysis and imaging of various lipid classes in negative ion mode.

EXPERIMENTAL SECTION

Synthesis of α-Cyanocinnamic Acid Derivatives.[33] Synthesis was done by Knoevenagel condensation: A mixture of cyanoacetic acid derivative (1.0 equiv), benzaldehyde derivative (0.9 equiv), and ammonium acetate (0.15 equiv) in toluene (20 mL) was refluxed for 2−6 h. After completion of reaction it was cooled to room temperature and recrystallized with an acetone/water or methanol/water mixture. In case of no precipitation the solvent was evaporated completely and then recrystallized.[34] The α-cyanoacetic acid amides were prepared by refluxing α-cyanoacetic acid ethyl ester with excess amine in ethanol as a solvent. All synthesized compounds were purified to homogeneity by repetitive recrystallization or column chromatography. The α-cyanocinnamic acid derivatives were characterized by ^{1}H and ^{13}C NMR spectroscopy and MALDI mass spectrometry (see Supporting Information).

MALDI-TOF Mass Spectrometry. Mass spectra were either acquired on an Autoflex III (355 nm SmartbeamTM laser; 200 Hz repetition rate, ~3×10^{-7} hPa) or an Ultraflex I (337 nm nitrogen laser; 25 Hz, ~10^{-7} hPa) (both from Bruker Daltonics, Bremen, Germany). The Smartbeam laser has a modulated beam profile. This needs to be taken into account whenever we refer to it as a 355 nm Nd:YAG laser throughout the text.

Autoflex III Parameters. Samples were analyzed in reflector mode with extraction at a source voltage of 19 kV and reflector voltage of 21 kV in both positive and negative ion mode. For comparison of matrix substances, laser energy thresholds [defined as laser intensity, for which an intensity of 1×10^4 arbitrary units (au) for the matrix ion peak was observed] were determined manually for each substance. For automated lipid measurements the AutoXecute function of the flexControl 3.0 software was used. Spectra were acquired in the mass range from m/z 400 to 2000 Da with a low mass gate at 370 and 390 Da for negative and positive ion mode, respectively; 4000 laser shots were accumulated per spot by random walk with 200 shots per position. The laser was set individually for each substance slightly above the threshold level to get the best intensity and signal-to-noise result. The MS was calibrated internally using a list of theoretical masses of detected lipids. Peak quality parameters were S/N ≥ 3, peak width < 0.2 Da at 80% peak intensity, and resolution > 1000. In case of 30 unsuccessful attempts, measurement was aborted. Spectra were determined with flexAnalysis 3.4 software (Bruker Daltonics).

Ultraflex I Parameters. Parameters were as used for Autoflex III, with the following exceptions: source and reflector voltages were 25 and 26.3 kV, respectively, in positive ion mode and 20 kV and 21 kV, respectively, in negative ion mode.

Statistical examination was done with Microsoft Excel. Average intensities and standard deviation were calculated of three replicates [Figures 3 and S2 and S3 (Supporting Information)]. To compare groups of spectra via gel view, spectra were analyzed using ClinProTools 2.2 software (Bruker Daltonics). Groups were generated from four single spectra [Figures 4 and S4 (Supporting Information)].

Determination of the $MSE_{lip.}$ Score.[35] To evaluate the matrix suppression effect (MSE), the $MSE_{lip.}$ score, defined as the summed analyte signals over the ion current from both matrix and analyte signals, in presence of 20 ng brain total lipid extract for the matrices 9-AA and Ph-CCA-NH_2 was calculated. Therefore, the number of matrix peaks ($\sum m$) with S/N ≥ 5 and the summed peaks derived from lipid extract ($\sum$lip.) with S/N ≥ 5 were determined in the presence of 20 ng extract for each matrix and the score was calculated: $MSE_{lip.} = \sum lip./(\sum lip. + \sum m)$.

MALDI-IMS. A frozen Sprague−Dawley rat brain was sliced into 10 μm coronal sections using a Leica CM1950 cryostat (Leica Biosystems, Nussloch, Germany) at a chamber temperature of −15 °C and a specimen head temperature of −11 °C. Cryosections were mounted onto indium tin oxide (ITO)-coated conductive glass slides (Bruker Daltonics, Bremen, Germany) and dried for 30 min under vacuum. Identical amounts of 9-AA [5 mg/mL in acetonitrile/water (80:20, v/v)] or Ph-CCA-NH_2 [5 mg/mL in acetone/water (90:10, v/v)] were deposited onto one piece of tissue, while the other was covered with a glass slide. For matrix deposition a SunCollect MALDI Spotter (SunChrom, Friedrichsdorf, Germany) was used. Air pressure was 2.5 bar. Matrix was deposited in nine layers, with medium flow rate set to 10 μL/min (first layer), 15 μL/min (second), 20 μL/min (third), and 25 μL/min (all others). The distance between tissue and spray head was 25.3 mm. MS images were obtained on the Autoflex III MALDI-TOF/TOF MS in negative ion-reflector mode in the m/z range from 600 to 1800 Da at a spatial resolution of 100 μm with 200 laser shots per position. Optimized laser energies for the two matrices, slightly above the individual threshold level, were determined before measurement and kept constant during one region. Regions with different matrix depositions were measured in random order (Figure 5, 9-AA region first; Figure S5, Supporting Information, Ph-CCA-NH_2 first) using flexImaging 3.0 software (Bruker Daltonics, Bremen, Germany). Mass filters were chosen with a width of 0.2 Da.

dx.doi.org/10.1021/ac4018154 | Anal. Chem. 2013, 85, 9156−9163

Normalization was passed. The MALDI-MS/MS analysis using the LIFT cell of the Autoflex III instrument was conducted directly on the tissue section after MALDI IMS.

ESI QqQ-MS/MS Measurements. Sprague–Dawley rat brain lipid raw extract was diluted for ESI QqQ-MS/MS analysis to a concentration corresponding to 0.31 mg wet weight per milliliter of methanol for negative mode MS and 0.31 mg wet weight per milliliter of methanol with 5 mM ammonium acetate for positive mode MS. All scans where performed on a Xevo TQ-S tandem mass spectrometer (Waters, Milford) by direct infusion with a flow rate of 20 μL min^{-1}. Scan time was 2 min with a scan duration of 3 s. All spectra were baseline corrected and smoothed with Savitzky–Golay algorithm twice with a window size of 3. Processing was done with MassLynks Software 4.1 (Waters, Milford).

RESULTS AND DISCUSSION

Rational Design and Spectroscopic Characterization of α-Cyanocinnamic Acid Derivatives. Absorption of

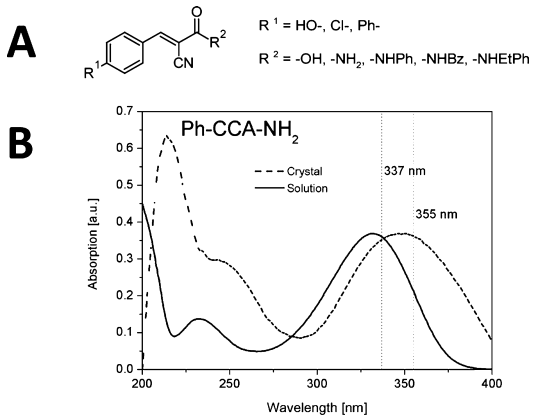

Figure 1. Structures of synthesized α-Cyanocinnamic acid derivatives and UV–vis absorption of new matrix Ph-CCA-NH$_2$. (A) Structures of synthesized α-cyanocinnamic acid derivatives (R^1-CCA-R^2) and (B) UV–vis absorption of Ph-CCA-NH$_2$ in solution [c = 624 μM in acetonitrile/water (4:1, v/v)] and in solid state ($A_{solution}$ = 0.91A_{solid}).

photons at the operational wavelength of the laser is an absolute requirement for any MALDI matrix. Since replacement of the hydroxyl group in HCCA against proton-affine substituents such as chlorine leads to a hypsochromic shift,[32] matrices like Cl-CCA are not very well suited for applications using MALDI-MS with frequency-tripled Nd:YAG lasers. Therefore, we sought to design novel cinnamic acid matrix compounds that avoided this hypsochromic shift and consequently could be useful in lipid analysis applications such as MALDI-IMS that today are often done with Nd:YAG lasers, in particular, Smartbeam lasers with a modulated beam profile. To this end, we used 4-chloro-α-cyanocinnamic acid (Cl-CCA), 4-hydroxy-α-cyanocinnamic acid (HCCA), and 4-phenyl-α-cyanocinnamic acid (Ph-CCA), which differ in their pK_a values, their molecular surface area (MSA), and hydrophobicity (clogP and clogD), as starting points for our design approach (Table S1, Supporting Information).

For analysis of lipids by MALDI-MS in negative ion mode, basic matrices such as 9-AA are preferred.[10,17] This matrix in particular features a relatively high clogP, which may enhance detection of hydrophobic lipid species. 9-AA has some drawbacks though, such as its unfavorable toxicology profile,[36]

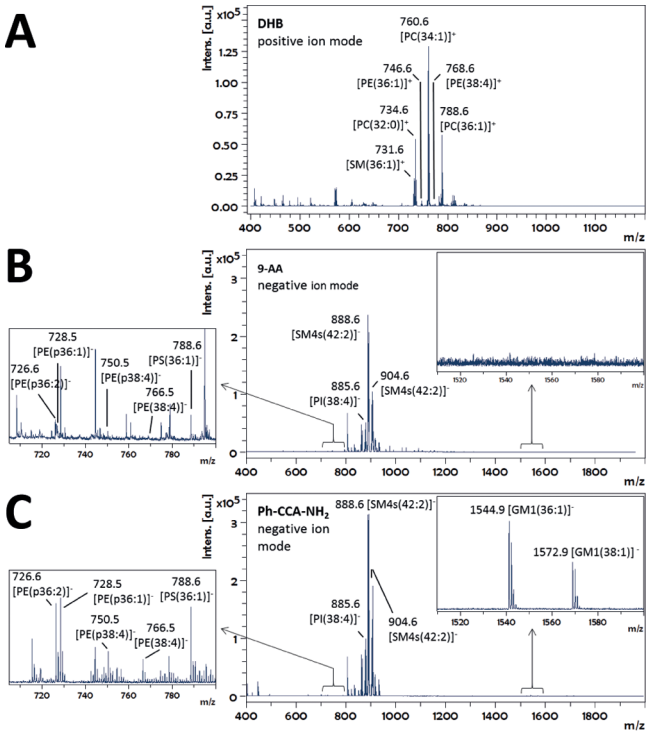

Figure 2. Brain total lipid extract is an adequate analyte for screening of a broad range of lipids. (A) MALDI-TOF MS spectra (modulated Nd:YAG laser) of brain total lipid extract in positive ion mode with DHB (0.5 M) in methanol or (B) in negative ion mode with 9-AA (5 mg/mL) in 2-propanol/acetonitrile (3:2, v/v) and accordingly (C) Ph-CCA-NH$_2$ (5 mg/mL) in acetonitrile/water (4:1, v/v).

often high variability in automated data acquisition (own unpublished observation), and an absorbance minimum at the laser irradiation wavelength, which leads to a high ionization energy threshold. Therefore, we used physicochemical properties of 9-AA like its clogP as guidance for the tailoring of cinnamic acid derivatives for negative ion mode measurements of lipid species. We furthermore reasoned that an acid functionality presumably would be counterproductive for deprotonation of analytes in negative ion mode. Therefore, the carboxyl functionality was replaced by neutral amides, to minimize the influence of matrix acid–base chemistry in the ionization process and to facilitate the detection of acid/base sensitive compounds. Use of different amide substituents for this replacement offered further opportunity to change the hydrophobicity of the compounds without changing the principle conjugated system for UV absorption in the MALDI process.

We synthesized 12 bisubstituted α-cyanocinnamic acid derivatives (R^1-CCA-R^2; Figure 1A) and measured their UV absorption in solution and solid state (Table S1B, Supporting Information). UV absorbance profiles of MALDI matrices can be determined as barium sulfate pellets or as sublimed films.[37,38] Solid-phase measurements, in general, show a broadening of absorbance bands. Furthermore, it was shown that oscillator strengths in solution and solid phase are comparable, when optical absorbance coefficients are determined of sublimed MALDI matrix films. Therefore, solution data can only be relied on within a factor of about 2 to provide data for modeling the solid film matrices.[38] In this work, we (re)crystallized matrix substances on a fiber optics to approximate conditions on a MALDI target plate. In summary,

dx.doi.org/10.1021/ac4018154 | Anal. Chem. 2013, 85, 9156–9163

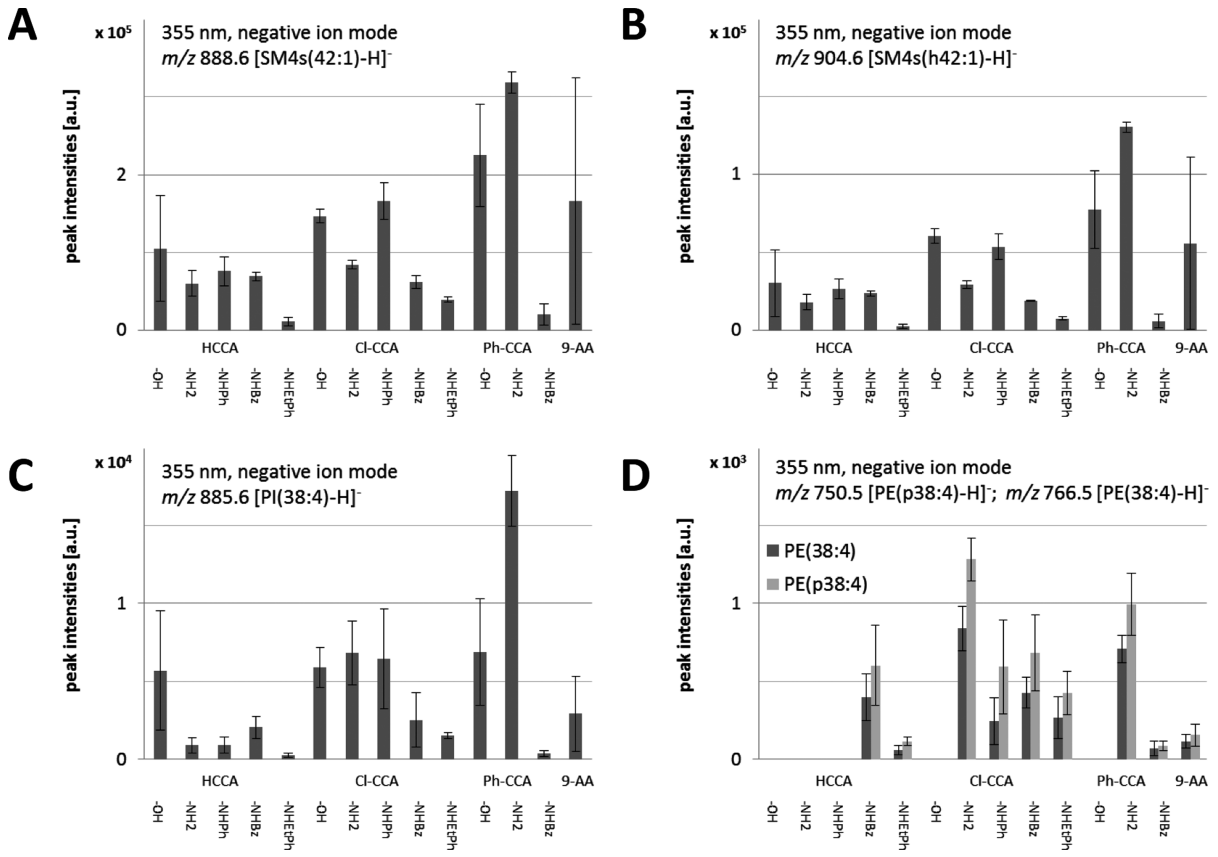

Figure 3. Ph-CCA-NH_2 is a versatile matrix with superior characteristics in negative ion mode. Mean peak intensities of selected lipids measured with 0.5 μg brain total lipid extract with α-cyanocinnamic acid matrices [5 mg/mL in acetonitrile/water (4:1, v/v)] or 9-AA [5 mg/mL in 2-propanol/acetonitrile (3:2, v/v)] in negative ion mode, measured with a Nd:YAG laser. Average intensities and standard deviation were calculated of three replicates. m/z values of negatively ionized lipids were (A) 888.6 $[SM4s(42:2) - H]^-$, (B) 904.6 $[SM4s(h42:2 - H)]^-$, (C) 885.6 $[PI(38:4) - H]^-$, and (D) 766.5 $[PE(38:4) - H]^-$ and 750.5 $[PE(p38:4) - H]^-$.

all α-cyanocinnamic acid derivatives showed UV-absorption in the solid state in the desired range of wavelengths. According to known UV/vis measurements of α-cyanocinnamic acid derivatives,[38,37] a more intense bathochromic shift as well as peak broadening was observed for the solid state measurements, as illustrated for Ph-CCA-NH_2 as an example (Figure 1B). Therefore, maximal absorption in the solid state is not reported as a fixed wavelength in Table S1B (Supporting Information), but as a range of maximal light absorption.

We next attempted automated evaluation of multiple matrices by MALDI-TOF MS. Although the variability of ion signals depends on laser irradiance (i.e., intensity, time and wavelength of laser irradiation), the main obstruction for automation was the inhomogeneity of the matrix surface.[39] We achieved more homogeneous crystallization by dissolving all HCCA derivatives in 80% acetonitrile, and then overlaying the air-dried lipid solution with them (i.e., PrimaDrop sample preparation method)[40] (Figure S1, Supporting Information). Crystal formation was still not uniform for all matrix substances. In some cases small crystals or needles were observed, but ring formation was avoided and automated data acquisition was possible.

Since we were interested in screening candidate matrix substances against a complex analyte mix containing a broad range of lipid classes, we tested brain total lipid extract and used DHB as a reference matrix for positive ion mode and 9-AA for negative ion mode MALDI-MS. The LIPID MAPS Database[41] was used for preliminary assignment of m/z values to lipids. Consistent with the literature for Sprague–Dawley rat brain,[42,43] m/z values of the most prominent peaks in positive ion mode corresponded to phosphatidyl choline (PC) isoforms {m/z 734.6, $[PC(32:0) + H]^+$; m/z 760.6, $[PC(34:1) + H]^+$; and m/z 788.6, $[PC(36:1) + H]^+$; Figure 2A}; peaks corresponding to sphingomyelin (SM) isoforms {m/z 731.6, $[SM(36:1) + H]^+$} and phosphatidyl ethanolamine (PE) species {m/z 746.6, $[PE(36:1) + H]^+$ and m/z 768.6, $[PE(38:4) + H]^+$} were also observed. Despite a 3-fold excess of PE over PC in the brain extract, PE detection was suppressed by PC in the extract,[44] resulting in very small signals. In negative ion mode MS spectra of brain lipid extract (Figure 2B,C), the most prominent lipids between m/z 400 and 2000 were hydroxylated (h) and nonhydroxylated sulfatides (SM4s isoforms) that are known to be selectively ionized by 9-AA with 355 nm laser,[16,17] whereas the same matrix substance appears to show no preference for a special lipid species in case of a nitrogen laser.[44,45] Nevertheless, signals of phospholipids such as phosphatidyl inositols (PI) and phosphatidyl serines (PS), negatively charged 1,2-diacyl-PE species (PE) and plasmalogenic (p) PE species as well as gangliosides (GM1) that occur in rat brain tissue[25,43,46] were also detected in brain total lipid extract, in particular with Ph-CCA-NH_2 matrix (Figure 2C). We concluded that this commercially available extract was a suitably complex analyte mix that was useful for matrix screening.

Semiautomated Screening of α-Cyanocinnamic Acid Amide Derivatives Reveals Ph-CCA-NH_2 as a Promising

dx.doi.org/10.1021/ac4018154 | Anal. Chem. 2013, 85, 9156–9163

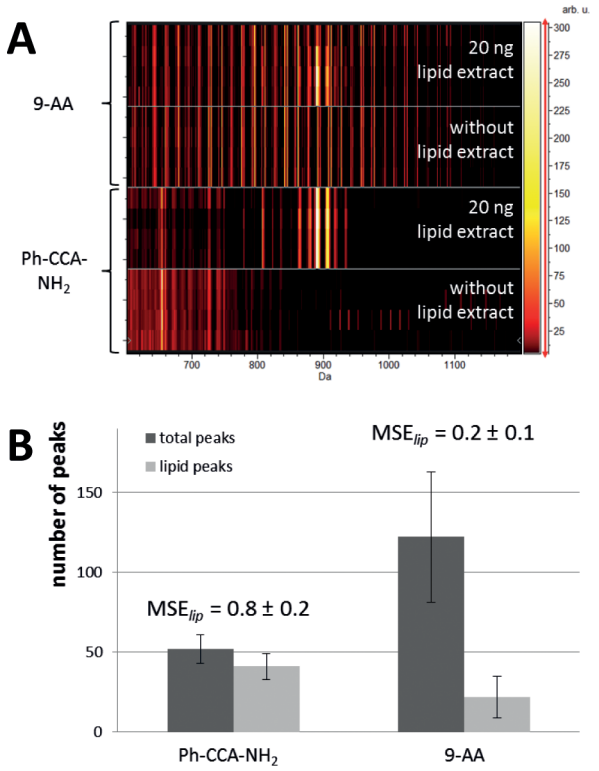

Figure 4. Reduced matrix noise and higher signal intensities result in a higher matrix suppression effect with Ph-CCA-NH_2. (A) Gel view of four groups of four negative ion MALDI spectra each. (Examples of single spectra are shown in Figure S4, Supporting Information.) Spectra were recorded with Ph-CCA-NH_2 (5 mg/mL in 90% acetone) matrix or 9-AA [5 mg/mL in 2-propanol/acetonitrile (3:2, v/v)] matrix. Matrix background spectra as well as spectra recorded with 20 ng of brain total lipid extract show less matrix noise in combination with Ph-CCA-NH_2 matrix. (B) Total number of peaks resulting from lipids signals and matrix background ($S/N \geq 5$) and number of lipid peaks ($S/N \geq 5$) with Ph-CCA-NH_2 or 9-AA. The $MSE_{lip.}$ score was calculated for both matrices in the presence of 20 ng of brain total lipid extract.

Negative Ion Matrix for Preferential Use with 355 nm Lasers. In order to take different laser thresholds of different α-cyanocinnamic acid amide derivatives into account, but to also avoid experimenter bias, the laser energy was set manually to a value slightly above the threshold level for each matrix and each MALDI instrument (for best intensity and signal-to-noise ratio) and data was then acquired automatically. The α-cyanocinnamic acid derivatives and reference matrices were compared by measuring the ion intensities of selected brain lipid extract species.

In the positive ion mode the intensities of lipid species PC(32:0), PC(34:1), and SM(36:1), generated with the α-cyanocinnamic acid derivatives and DHB as reference, were compared (Figure S2, Supporting Information). Since the comparison of absolute intensities between two different MALDI instruments at two sites is not useful, the patterns of relative ion intensities were considered for the respective instruments. From this, HCCA-NH_2 showed promise for lipid detection in positive ion mode primarily when combined with a 355 nm Smartbeam laser. This matrix displayed an improved signal intensity for SM(36:1) (Figure S2B, Supporting Information) and comparable intensities for PC species (vs DHB). In addition, comparable performances of Cl-CCA and DHB, well-known for detection of DPPC in positive ion mode,[47] were confirmed with PC species in brain total lipid extract (Figure S2A/C, Supporting Information). The sulfatides SM4s(42:2) and SM4s(h42:2) as well as phospholipids PI(36:4), PE(38:4), and PE(p38:4) were chosen as exemplary lipids in negative ion mode. As expected, 9-AA with a Nd:YAG laser resulted in high, but variable, signal intensities for sulfatides, but it did not work well for phospholipids (Figure 2B and 3). Furthermore, all cinnamic acid derivatives displayed matrix properties for lipids in negative ion mode. Taking all measurements with a 355 nm laser together (Figure 3A-D), Ph-CCA-NH_2 is always a good matrix and sometimes the best, suggesting broad applicability of Ph-CCA-NH_2 in lipid MALDI MS, because of the outstanding intensity for PI as well as good results for sulfatides and the less intense PE species.

Whereas the comparison of both lasers showed a comparable trend in positive ion mode, the intensity pattern with nitrogen laser in negative ion was very different (Figure S3, Supporting Information). Surprisingly, measurements at 337 nm with the newly synthesized α-cyanocinnamic acid derivatives resulted in relatively low ion intensities compared with 9-AA. Consequently, for detection of negatively charged lipids with nitrogen laser MALDI instruments, 9-AA matrix may still be advised.

Overall, our screening results suggested that, in line with UV measurements in the solid state, most of the α-cyanocinnamic acid amide derivatives we synthesized had MALDI matrix properties for lipids and that their lipid preference and selectivity warrant further investigation. Replacement of the carboxyl with an amide group had no negative effect on matrix performance, with the α-cyanocinnamic acid amides HCCA-NH_2 and particularly Ph-CCA-NH_2 yielding promising results with a Smartbeam laser.

Ph-CCA-NH_2 Displays Higher Matrix Suppression and Higher Versatility in Negative Ion MALDI-IMS. Desorption and ionization of matrix molecules during analyte detection causes background peaks in the low-mass region ($m/z < 1000$) because of matrix fragmentation and cluster formation. These background signals can be suppressed by sufficient analyte ions.[48,49] It has been noted that this matrix suppression effect (MSE) is not observed with all matrices at the same ratio and is generally reduced if the crystallization is inhomogeneous.[49] Besides the matrix:analyte ratio, the most adjustable factor is laser intensity. The MSE is maximal near the MALDI laser intensity threshold, because a stronger laser pulse generates more matrix ions that require more analytes to quench them. Nevertheless, it is practically impossible to prepare samples with an appropriate matrix:analyte ratio, since the analyte concentrations in biological samples are often unknown. To circumvent this limitation, it is desirable that the matrix of choice already promotes the MSE at low amounts of sample.

Bearing the MSE in mind, we examined formation of background matrix signals and their suppression by the matrices Ph-CCA-NH_2 and 9-AA near their laser intensity thresholds in the absence or presence of 20 ng of brain total lipid extract (Figure 4A). In the absence of lipid extract, characteristic matrix cluster formation was observed in the case of 9-AA, whereas the matrix spectra of Ph-CCA-NH_2 showed fewer background signals (Figures 4A and Figure S4B, Supporting Information). The majority of the latter were suppressed in the presence of lipid extract. This MSE was not observed in the case of 9-AA matrix with 20 ng of lipid extract (Figure S4A, Supporting Information). The $MSE_{lip.}$ score with

dx.doi.org/10.1021/ac4018154 | Anal. Chem. 2013, 85, 9156−9163

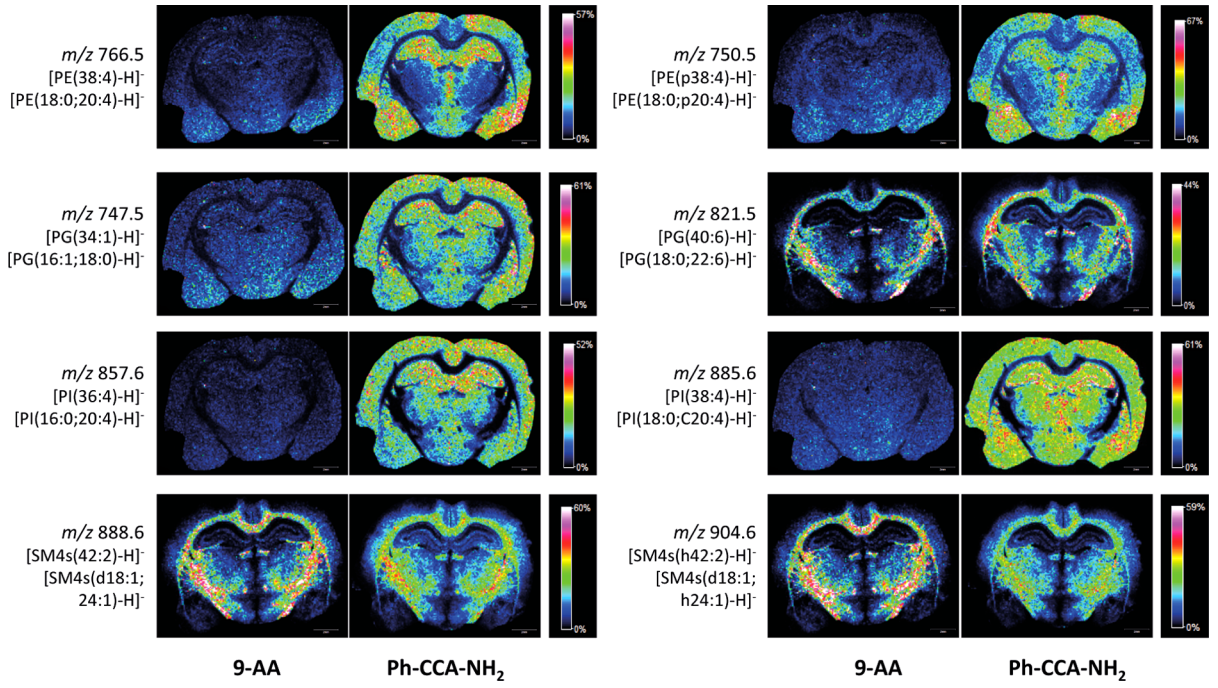

Figure 5. Ph-CCA-NH_2 matrix enables MALDI-IMS of various lipid species. Imaging was performed on two adjacent cryosections of Sprague–Dawley rat brain on the same ITO slide. Data was acquired in negative ion-reflector mode at a spatial resolution of 100 μm with 200 laser shots per position. Prior to measurement, the same amount of 9-AA [5 mg/mL in acetonitrile/water (80:20, v/v)] (left side) or Ph-CCA-NH_2 [5 mg/mL in acetone/water (90:10, v/v)] (right side) was deposited onto one of the tissue sections with a SunCollect MALDI spotter. Imaging was carried out while the laser energy was kept constant and slightly above the individual threshold level for one region. The 9-AA region was measured first. Mass filters were chosen with a width of 0.2 Da.

20 ng extract was 4 times improved with Ph-CCA-NH_2 when compared to 9-AA (Figure 4B).

We therefore reasoned that the small number of background peaks in the m/z range 400–2000 may imply that Ph-CCA-NH_2 be useful in the combined detection of sulfatides and other lipids in IMS experiments. We therefore acquired two independent IMS data sets using rat brain cryosections. In both of them one piece of tissue was coated with 9-AA and the other with Ph-CCA-NH_2. In one experiment the 9-AA-coated region was measured first (Figure 5), in the other it was measured last (Figure S5, Supporting Information). The images were in good agreement with the intensities displayed in Figure 3. The reported selectivity of 9-AA for sulfatides [SM4s(42:2) and SM4s(h42:2)] was confirmed.[17,21] In contrast, Ph-CCA-NH_2 also enabled imaging and localizing other lipids such as phosphatidyl inositols [e.g., PI(36:4) and PI(38:4)] and even the phosphatidyl ethanolamines [PE(38:4) and PE(p38:4)] or the phosphatidyl glycerol species [PG(34:1) and PG(40:6)]. For further validation of the identity of lipids represented in Figures 5 and S5 (Supporting Information), on tissue MS/MS spectra were acquired for the above-named lipid isoforms with Ph-CCA-NH_2 matrix (Table S2, Supporting Information). Hereby, m/z 885.6 was identified as $[PI(18:0;20:4) - H]^-$ and m/z 821.5 as $[PG(18:0;22:6) - H]^-$. The other assignments are illustrated in Table S2 (Supporting Information).[50] On tissue MS/MS fragmentation with 9-AA was only possible for sulfatides and for PI(18:0;20:4), whereas no difference in the fragmentation pattern generated with either Ph-CCA-NH_2 or 9-AA was observed, as exemplified for $[PI(18:0;20:4) - H]^-$ (m/z 885.6) (Figure S6, Supporting Information). In general, the wide precursor ion selector window of the Autoflex III MS complicates fragmentation analysis. For less intense signals the selector window range has to be expanded. Hence, fragmentation of other lipids is possible. Consequently, the unambiguous assignment of m/z 821.6 in the case of 9-AA matrix was not possible, although a distinct image was obtained. To confirm that the named lipids, to which imaged m/z values had been matched, were indeed present in rat brain, we analyzed crude extract of the corresponding rat brain region by ESI-QqQ-MS/MS in a series of precursor and neutral loss scanning experiments (Figure 6), demonstrating the presence of all lipids imaged with Ph-CCA-NH_2.

■ CONCLUSION

In this study, with the goal of identifying a novel matrix for lipid MALDI-IMS applications, we have conducted a semiautomated comparison of different α-cyanocinnamic acid amide derivatives (R^1-CCA-R^2) using brain total lipid extract as analyte containing a broad spectrum of lipids. Automated measurement was installed to avoid experimenter bias. The homogeneous crystallization necessary for such measurements could be achieved by PrimaDrop sample preparation. Comparison of different matrix substances demonstrated that replacement of the carboxyl group with an amide group is a promising method to improve matrix performance for lipids. Superior to any other matrix tested in this study in negative ion mode with 355 nm Smartbeam laser, 4-phenyl-α-cyanocinnamic acid amide displayed features of MALDI matrix with improved sensitivity and reproducibility and a small number of background peaks in the mass range of lipids. In conclusion, Ph-CCA-NH_2 may be an attractive alternative matrix of choice for negative ion mode detection of various less abundant lipids by MALDI-MS.

dx.doi.org/10.1021/ac4018154 | Anal. Chem. 2013, 85, 9156–9163

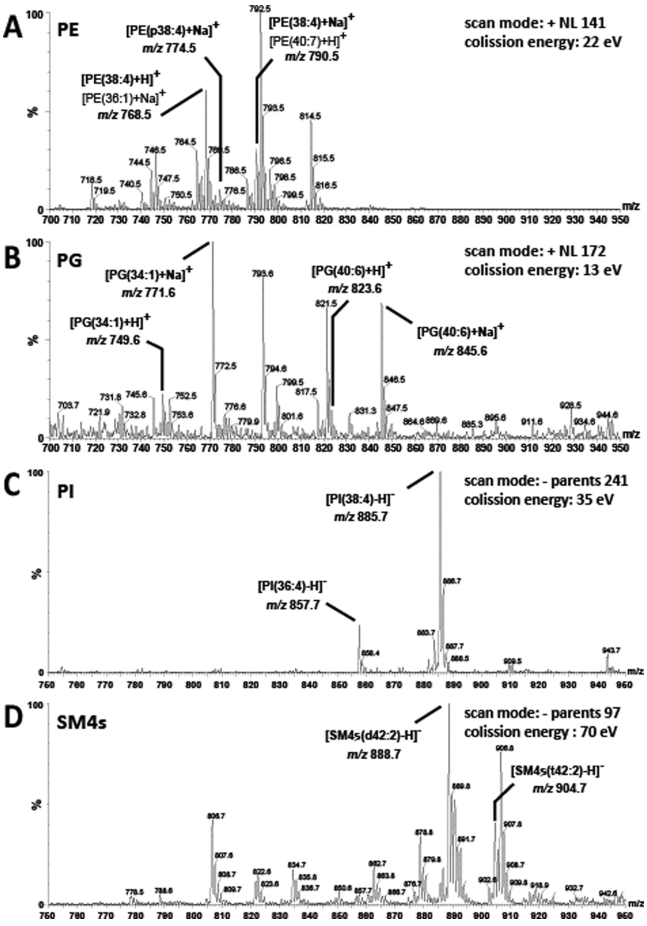

Figure 6. Validation of molecular peak assignment in MALDI-IMS by ESI QqQ-MS/MS. Identification of all lipid species assigned in MALDI IMS (Figure 5) in rat brain raw extract either by specific neutral-loss (NL) scanning in positive ion mode for (A) PE (+NL 141) and (B) PG (+NL 172) or by specific parent ion scanning in negative ion mode for (C) PI (− parents 241) and (D) SM4s (− parents 97).

■ ASSOCIATED CONTENT

Ⓢ Supporting Information

Additional information as noted in the text. This material is available free of charge via the Internet at http://pubs.acs.org.

■ AUTHOR INFORMATION

Corresponding Author

*E-mail: c.hopf@hs-mannheim.de. Phone: +49 (0)621/292-6802. Fax: +49 (0)621/292-6420.

Notes

The authors declare no competing financial interest.

■ ACKNOWLEDGMENTS

This work was supported by the Baden-Württemberg Ministry of Science and Culture (INST 874/2-1 LAGG to C.H.), by a joined grant ("ZAFH ABIMAS") from ZO IV by the Landesstiftung Baden-Württemberg and the Europäischer Fonds für regionale Entwicklung (EFRE; to H.D.J., R.S., and C.H.), and by a grant by the Phospholipid-Forschungszentrum e.V., Heidelberg, Germany (to C.H.).

■ REFERENCES

(1) Phillips, R.; Ursell, T.; Wiggins, P.; Sens, P. *Nature* **2009**, *459*, 379−85.
(2) O'Donnell, V. B.; Murphy, R. C. *Blood* **2012**, *120*, 1985−92.
(3) Brewer, J. W. *Biochim. Biophys. Acta* **2013**, *1831*, 642−51.
(4) Vance, J. E.; Tasseva, G. *Biochim. Biophys. Acta* **2013**, *1831*, 543−54.
(5) Han, X.; Yang, K.; Gross, R. W. *Mass Spectrom. Rev.* **2012**, *31*, 134−78.
(6) Harkewicz, R.; Dennis, E. A. *Annu. Rev. Biochem.* **2011**, *80*, 301−25.
(7) Karas, M.; Hillenkamp, F. *Anal. Chem.* **1988**, *60*, 2299−301.
(8) Stoeckli, M.; Farmer, T. B.; Caprioli, R. M. *J. Am. Soc. Mass Spectrom.* **1999**, *10*, 67−71.
(9) Spengler, B.; Hubert, M. *J. Am. Soc. Mass Spectrom.* **2002**, *13*, 735−48.
(10) Fuchs, B.; Suss, R.; Schiller, J. *Prog. Lipid Res.* **2010**, *49*, 450−75.
(11) Gode, D.; Volmer, D. A. *Analyst* **2013**, *138*, 1289−315.
(12) Fernandez, J. A.; Ochoa, B.; Fresnedo, O.; Giralt, M. T.; Rodriguez-Puertas, R. *Anal. Bioanal. Chem.* **2011**, *401*, 29−51.
(13) Colsch, B.; Jackson, S. N.; Dutta, S.; Woods, A. S. *ACS Chem. Neurosci.* **2011**, *2*, 213−22.
(14) Woods, A. S.; Colsch, B.; Jackson, S. N.; Post, J.; Baldwin, K.; Roux, A.; Hoffer, B.; Cox, B. M.; Hoffer, M.; Rubovitch, V.; Pick, C. G.; Schultz, J. A.; Balaban, C. *ACS Chem. Neurosci.* **2013**, *4*, 594−600.
(15) Tholey, A.; Heinzle, E. *Anal. Bioanal. Chem.* **2006**, *386*, 24−37.
(16) Cheng, H.; Sun, G.; Yang, K.; Gross, R. W.; Han, X. *J. Lipid Res.* **2010**, *51*, 1599−609.
(17) Marsching, C.; Eckhardt, M.; Grone, H. J.; Sandhoff, R.; Hopf, C. *Anal. Bioanal. Chem.* **2011**, *401*, 53−64.
(18) Karas, M.; Bachmann, D.; Hillenkamp, F. *Anal. Chem.* **1985**, *57*, 2935−9.
(19) Zenobi, R.; Knochenmuss, R. *Mass Spectrom. Rev.* **1998**, *17*, 337−66.
(20) Wang, H. Y.; Jackson, S. N.; Post, J.; Woods, A. S. *Int. J. Mass Spectrom.* **2008**, *278*, 143−9.
(21) Cerruti, C. D.; Benabdellah, F.; Laprevote, O.; Touboul, D.; Brunelle, A. *Anal. Chem.* **2012**, *84*, 2164−71.
(22) Rujoi, M.; Estrada, R.; Yappert, M. C. *Anal. Chem.* **2004**, *76*, 1657−63.
(23) Bouschen, W.; Spengler, B. *Int. J. Mass Spectrom.* **2007**, *266*, 129−37.
(24) Schiller, J.; Suss, R.; Fuchs, B.; Muller, M.; Petkovic, M.; Zschornig, O.; Waschipky, H. *Eur. Biophys. J.* **2007**, *36*, 517−27.
(25) Jackson, S. N.; Wang, H. Y.; Woods, A. S. *J. Am. Soc. Mass Spectrom.* **2007**, *18*, 17−26.
(26) Jackson, S. N.; Wang, H. Y.; Woods, A. S.; Ugarov, M.; Egan, T.; Schultz, J. A. *J. Am. Soc. Mass Spectrom.* **2005**, *16*, 133−8.
(27) Lorkiewicz, P.; Cecilia Yappert, M. *J Mass Spectrom.* **2009**, *44*, 137−43.
(28) Astigarraga, E.; Barreda-Gomez, G.; Lombardero, L.; Fresnedo, O.; Castano, F.; Giralt, M. T.; Ochoa, B.; Rodriguez-Puertas, R.; Fernandez, J. A. *Anal. Chem.* **2008**, *80*, 9105−14.
(29) Wang, H. Y.; Jackson, S. N.; Woods, A. S. *J. Am. Soc. Mass Spectrom.* **2007**, *18*, 567−77.
(30) Teuber, K.; Schiller, J.; Fuchs, B.; Karas, M.; Jaskolla, T. W. *Chem. Phys. Lipids* **2010**, *163*, 552−60.
(31) Shroff, R.; Rulisek, L.; Doubsky, J.; Svatos, A. *Proc. Natl. Acad. Sci U. S. A.* **2009**, *106*, 10092−6.
(32) Jaskolla, T. W.; Lehmann, W. D.; Karas, M. *Proc. Natl. Acad. Sci. U. S. A.* **2008**, *105*, 12200−5.
(33) Cope, A. C. *J. Am. Chem. Soc.* **1937**, *59*, 2327−30.
(34) Jaskolla, T.; Karas, M. Patent in http://www.patent-de.com/20090108/DE102007040251B3.html, 2009.
(35) McCombie, G.; Knochenmuss, R. *Anal. Chem.* **2004**, *76*, 4990−7.
(36) Sakore, T. D.; Jain, S. C.; Tsai, C. C.; Sobell, H. M. *Proc. Natl. Acad. Sci. U. S. A.* **1977**, *74*, 188−92.

(37) Soltwisch, J.; Jaskolla, T. W.; Hillenkamp, F.; Karas, M.; Dreisewerd, K. *Anal. Chem.* **2012**, *84*, 6567−76.
(38) Allwood, D. A.; Dreyfus, R. W.; Perera, I. K.; Dyer, P. E. *Rapid Commun. Mass Spectrom.* **1996**, *10*, 1575−8.
(39) Jensen, O. N.; Mortensen, P.; Vorm, O.; Mann, M. *Anal. Chem.* **1997**, *69*, 1706−14.
(40) Ruh, H.; Sandhoff, R.; Meyer, B.; Gretz, N.; Hopf, C. *Anal. Chem.* **2013**, *85*, 6233−40.
(41) Fahy, E.; Cotter, D.; Sud, M.; Subramaniam, S. *Biochim. Biophys. Acta, Mol. Cell Biol. Lipids* **2011**, *1811*, 637−47.
(42) Jackson, S. N.; Wang, H. Y.; Woods, A. S. *J. Am. Soc. Mass Spectrom.* **2005**, *16*, 2052−6.
(43) Jackson, S. N.; Wang, H. Y.; Woods, A. S. *Anal. Chem.* **2005**, *77*, 4523−7.
(44) Petković, M.; Schiller, J.; Müller, M.; Benard, S.; Reichl, S.; Arnold, K.; Arnhold, J. *Anal. Biochem.* **2001**, *289*, 202−16.
(45) Fuchs, B.; Bischoff, A.; Suss, R.; Teuber, K.; Schurenberg, M.; Suckau, D.; Schiller, J. *Anal. Bioanal. Chem.* **2009**, *395*, 2479−87.
(46) Woods, A. S.; Jackson, S. N. *AAPS J.* **2006**, *8*, E391−5.
(47) Jaskolla, T.; Fuchs, B.; Karas, M.; Schiller, J. *J. Am. Soc. Mass Spectrom.* **2009**, *20*, 867−74.
(48) Knochenmuss, R.; Dubois, F.; Dale, M. J.; Zenobi, R. *Rapid Commun. Mass Spectrom.* **1996**, *10*, 871−7.
(49) Knochenmuss, R.; Karbach, V.; Wiesli, U.; Breuker, K.; Zenobi, R. *Rapid Commun. Mass Spectrom.* **1998**, *12*, 529−34.
(50) Hsu, F. F.; Turk, J. *J. Am. Soc. Mass Spectrom.* **2000**, *11*, 986−99.